Effects of Cooper minima in resonance enhanced multiphoton ionization-photoelectron spectroscopy of NO via the D 2Σ+ and C 2Π Rydberg states

Kwanghsi Wang, J. A. Stephens, and V. McKoy

Citation: The Journal of Chemical Physics **95**, 6456 (1991); doi: 10.1063/1.461542
View online: http://dx.doi.org/10.1063/1.461542
View Table of Contents: http://scitation.aip.org/content/aip/journal/jcp/95/9?ver=pdfcov
Published by the AIP Publishing

Effects of Cooper minima in resonance enhanced multiphoton ionization-photoelectron spectroscopy of NO via the $D\,^2\Sigma^+$ and $C\,^2\Pi$ Rydberg states

Kwanghsi Wang, J. A. Stephens, and V. McKoy
Arthur Amos Noyes Laboratory of Chemical Physics,[a] *California Institute of Technology, Pasadena, California 91125*

(Received 20 June 1991; accepted 15 July 1991)

Cooper minima are predicted to occur in the $3p\sigma \rightarrow k\sigma(l=2)$ and $3p\sigma \rightarrow k\pi(l=2)$ channels in the resonance enhanced multiphoton ionization of NO via the $D\,^2\Sigma^+(3p\sigma)$ Rydberg state. The low energy $k\sigma(l=2)$ Cooper minimum leads to the observed $\Delta N = N^+ - N' = 0$ photoelectron peak, in addition to the $\Delta N = \pm 1, \pm 3$ peaks seen in the rotational spectra. The Cooper minima are accompanied by significant l mixing in the continuum due to the nonspherical molecular potential and result in a strong dependence of rotational branching ratios and angular distributions on photoelectron kinetic energy. A Cooper minimum is also predicted in the $3p\pi \rightarrow k\delta(l=2)$ channel for photoionization of the $C\,^2\Pi(3p\pi)$ Rydberg state. The effect of this Cooper minimum on photoelectron spectra and photoelectron angular distributions is also investigated.

I. INTRODUCTION

Resonance enhanced multiphoton ionization-photoelectron spectroscopy (REMPI-PES) of molecules has become a powerful tool for probing the characteristics of intermediate electronic states and the dynamics of excited-state photoionization.[1-3] The REMPI-PES technique has been employed successfully in studies of several diatomic molecules (e.g., NO, H_2, D_2, CO, N_2, O_2, I_2).[1-19] In many of these cases, the photoelectron detection scheme had insufficient energy resolution to distinguish the outgoing photoelectron associated with a specific rotational level of the molecular ion. Important exceptions are the pioneering studies by Müller-Dethlefs *et al.*[9] and Sander *et al.*[10] who achieved an energy resolution of less than 1 cm^{-1} by using the zero-kinetic-energy (ZEKE) technique, by Reilly and coworkers[4-7] who investigated REMPI of NO via the $A\,^2\Sigma^+(3s\sigma)$, $C\,^2\Pi(3p\pi)$, and $D\,^2\Sigma^+(3p\sigma)$ Rydberg states, and by Allendorf *et al.*[8] who studied $(1+1')$ REMPI rotational branching ratios and photoelectron angular distributions of NO via the $A\,^2\Sigma^+(3s\sigma)$ state. These rotationally resolved photoelectron energy distributions and associated photoelectron angular distributions have stimulated a number of *ab initio* studies.[20-25]

Parity selection rules,[20,26-28] which govern the changes of rotational angular momentum $\Delta N = N^+ - N'$, with N^+ and N' the rotational quantum numbers of the ionic and intermediate states, respectively, have been emphasized throughout these studies both experimentally and theoretically. For example, they correctly account for the dominant $\Delta N = 0$ peak and the weaker $\Delta N = \pm 1, \pm 2$ peaks seen in $(1+1')$ REMPI of NO via the $A\,^2\Sigma^+(3s\sigma)$ Rydberg state[4-6,8,9,20] and the $\Delta N = 0, \pm 2$ (*ee* line) and $\Delta N = \pm 1, \pm 3$ (*ff* line) propensities in photoionization of different parity components of the $C\,^2\Pi(3p\pi)$ Rydberg state[5] in $(2+1)$ REMPI experiments. However, in the $(2+1)$ REMPI of NO via the $D\,^2\Sigma^+(3p\sigma)$ state,[4,21,22] an intense and unexpected $\Delta N = 0$ peak was observed in addition to the anticipated $\Delta N = \pm 1, \pm 3$ peaks. According to the propensity rule, this unusual peak should derive predominantly from odd partial waves, particularly $l = 1$ (p-wave). On the other hand, self-consistent field (SCF) calculations show that the Rydberg orbital of the $D\,^2\Sigma^+(3p\sigma)$ state contains only a small amount of s or d character.[5,7,29] An atomiclike propensity rule, which would predict $l = 0$ and $l = 2$ character for the photoelectron, i.e., $l = l_0 \pm 1$, where l_0 is a partial wave component of the Rydberg electron, thus seems wholly inadequate. Theoretical studies initially attributed this $\Delta N = 0$ peak to essentially l mixing in the continuum which gave rise to a significant $l = 1$ photoelectron matrix element.[22] In a recent $(1+1')$ REMPI-PES study, it was further argued that coupling between vibronic levels of the $A\,^2\Sigma^+(v=4)$ and $D\,^2\Sigma^+(v=0)$ Rydberg states also contributed to the observed intensity of this $\Delta N = 0$ peak.[7]

In the present work, we reexamine the ion rotational distributions seen in $(2+1)$ REMPI of NO via this $D\,^2\Sigma^+(3p\sigma)$ state and demonstrate that a Cooper minimum[30-38] around 0.33 eV in the $3p\sigma \rightarrow k\sigma(l=2)$ photoionization channel plays a crucial role in determining the observed $\Delta N = 0$ peak. In fact, it is the depression of the $l = 2$ wave and subsequent enhancement of the relative contribution of $l = odd$ waves brought on by this low-energy Cooper minimum that results in the unusual $\Delta N = 0$ peak in the ion rotational distribution and the dependence of the rotational branching ratios on photoelectron energy. Our *ab initio* calculations predict that Cooper minima exist in the

[a] Contribution No. 8464.

 0021-9606/91/216456-07$03.00

$3p\sigma \rightarrow k\sigma(l=2)$ and $3p\sigma \rightarrow k\pi(l=2)$ channels for photoionization of the $D\,^2\Sigma^+(3p\sigma)$ Rydberg state. Rudolph *et al.*[39] have previously identified the $3p\sigma \rightarrow k\pi$ Cooper minimum in NO $D\,^2\Sigma^+$ ionization and showed that it results in a marked change in sign in the circular dichroism in the photoelectron angular distribution. These Cooper minima in NO are similar to those found in the $3p\sigma \rightarrow k\pi$ transitions in REMPI via the $D\,^2\Sigma^-(3p\sigma)$ state of OH[35,36] and the $3\,^3\Pi(3p\sigma)$ state of NH.[37] Recently it has also been shown in rotationally resolved REMPI-PES spectra via the $D\,^2\Sigma^-(3p\sigma)$ of OH that the Cooper minimum results in a primarily $\Delta N = even$ distribution (with $\Delta N = 0$ most intense), in contrast to a $\Delta N = odd$ distribution expected for the photoionization of the $D\,^2\Sigma^-(3p\sigma)$ state.[38] Cooper minima in the $(2+1')$ REMPI spectra via the $H\,^2\Sigma^+(3d,4s)$ state have been seen to have marked effects on the rotational branching ratios as the photoelectron matrix elements change partial wave character around the Cooper minimum.[40] Cooper minima predicted via the $H\,^2\Sigma^+(3d,4s)$ state occur at approximately the same photoelectron kinetic energy (2.6 eV in the $k\sigma$ and 2.9 eV in the $k\pi$ channels) which allows production of molecular ions in a specific rotational level; however, those predicted via the $D\,^2\Sigma^+(3p\sigma)$ state occur at quite *different* kinetic energies (0.33 eV in the $k\sigma$ and 3.2 eV in the $k\pi$ channels). A Cooper minimum has also been identified in the optical–optical double resonance spectra via the $C\,^2\Pi(3p\pi)$ Rydberg state of NO.[41] However, no Cooper minimum has been found in photoionization of the $A\,^2\Sigma^+(3s\sigma)$ state within the ~0–10 eV kinetic energy range studied.

In this paper, we systematically investigate how these newly identified Cooper minima affect the rotational branching ratios and photoelectron angular distributions in $(2+1')$ REMPI via the $D\,^2\Sigma^+$ and $C\,^2\Pi$ Rydberg states of NO. The photoelectron energy dependence of rotational branching ratios and angular distributions are examined, including amplitudes of relevant photoelectron matrix elements. Additionally, in light of the presence of these Cooper minima, we have reexamined the ionic rotational branching ratios in the $(2+1)$ REMPI of NO via the $D\,^2\Sigma^+(3p\sigma)$ state in more extensive calculations. The resulting branching ratios show a significantly stronger $\Delta N = 0$ peak for photoelectron detection parallel to the laser polarization than seen in earlier studies.[21,22] Details of our studies of the $(2+1)$ REMPI-PES for the $C\,^2\Pi$ state of NO and comparison with experiment are reported elsewhere.[42]

II. THEORY AND CALCULATIONAL DETAILS

$(2+1')$ REMPI processes via the $D\,^2\Sigma^+(3p\sigma)$ and $C\,^2\Pi(3p\pi)$ intermediate Rydberg states of NO are summarized as follows:

$$\mathrm{NO}[X\,^2\Pi(v_0=0,J_0)] \xrightarrow{2\omega} \mathrm{NO}^*[D\,^2\Sigma^+(v=0,J,N)] \xrightarrow{\omega'} \mathrm{NO}^+[X\,^1\Sigma^+(v^+,J^+=N^+)] + e^-(\mathbf{k}), \quad (1a)$$

$$\mathrm{NO}[X\,^2\Pi(v_0=0,J_0)] \xrightarrow{2\omega} \mathrm{NO}^*[C\,^2\Pi(v=0,J)] \xrightarrow{\omega'} \mathrm{NO}^+[X\,^1\Sigma^+(v^+,J^+=N^+)] + e^-(\mathbf{k}). \quad (1b)$$

They are viewed as two-step processes with a two-photon absorption from an initially unaligned $X\,^2\Pi$ ground state (all M_{J_0} levels equally populated) to the $D\,^2\Sigma^+$ or $C\,^2\Pi$ resonant intermediate state, followed by subsequent one-photon absorption from the aligned intermediate state to the ionization continuum. The frequency ω' differs from ω in a two-color experiment. Under collision-free conditions, each M_J channel can be treated as an independent ionization channel for linearly polarized light. Therefore, the differential cross section for photoionization of the resonant state by the third photon can be written as

$$\frac{d\sigma}{d\Omega} = \sum_{M_J,M_{J^+}} \rho_{M_JM_J} |\Gamma_{M_JM_{J^+}}|^2 = \sum_{L=0}^{L_{\max}/2} \beta_{2L} P_{2L}(\cos\theta), \quad (2)$$

where σ is the total cross section, $P_L(\cos\theta)$ the Lth Legendre polynomial, $L_{\max}=6$, $|\Gamma_{M_JM_{J^+}}|^2$ the ionization probability out of the M_J magnetic sublevel, and $\rho_{M_JM_J}$ its population. An expression for $\Gamma_{M_JM_{J^+}}$ within Hund's case (b) coupling scheme, which is suitable for the $D\,^2\Sigma^+$ intermediate state, has been given in Ref. 26. However, the $C\,^2\Pi$ state with its spin–orbit splitting constant $A = 3.0\ \mathrm{cm}^{-1}$ and rotational constant $B = 2.0\ \mathrm{cm}^{-1}$ is best described by the intermediate coupling scheme between Hund's cases (a) and (b).[43] The expressions for $\Gamma_{M_JM_{J^+}}$ with the intermediate coupling scheme has been recently given by Wang and McKoy.[28] For $^2\Sigma^+$ intermediate states, an incoherent sum over allowed J levels is needed to account for the mixed rotational branches with $J = N \pm \frac{1}{2}$. For the low intensity experiments of interest here, $\rho_{M_JM_J}$ has the general form for two-photon excitation

$$\rho_{M_JM_J} \propto \left| \sum_{kp} \begin{pmatrix} J & 1 & J_{kp} \\ -M_J & 0 & M_J \end{pmatrix} \begin{pmatrix} J_{kp} & 1 & J_0 \\ -M_J & 0 & M_J \end{pmatrix} B_{kp} \right|^2, \quad (3)$$

where J_{kp} is the total angular momentum of a dipole-allowed virtual state $|k\rangle$ of the pth transition path and B_{kp} is related to the rotational line strength.[44] Evaluation of Eq. (3) in general requires summation over all dipole-allowed virtual states $|k\rangle$ and possible transition paths p. For rotational branches other than the Q branch, Eq. (3) can be further simplified into a product of a 3-j symbol and rotational line strength B,[45]

$$\rho_{M_JM_J} \propto \begin{pmatrix} J & 2 & J_0 \\ -M_J & 0 & M_J \end{pmatrix}^2 B. \quad (4)$$

However, in the case of a Q branch, evaluation of $\rho_{M_JM_J}$ requires two factors B_0 and B_2,[44]

$$\rho_{M_JM_J} \propto \left| \begin{pmatrix} J & 2 & J_0 \\ -M_J & 0 & M_J \end{pmatrix} B_2 + B_0 \right|^2. \quad (5)$$

Note that B_0 contains no polarization information, but is crucial in determining the alignment $\rho_{M_JM_J}$ of the intermediate state for $(2+1')$ REMPI via the Q rotational branch.

The photoelectron signal detected along the polarization direction of the laser is given by $\beta_0+\beta_2+\beta_4+\beta_6$ and the perpendicular signal by $\beta_0-\frac{1}{2}\beta_2+\frac{3}{8}\beta_4-\frac{5}{16}\beta_6$.

The wave functions for the $D\,^2\Sigma^+(3p\sigma)$ state with electron configuration $1\sigma^2 2\sigma^2 3\sigma^2 4\sigma^2 5\sigma^2 1\pi^4 7\sigma$ and the $C\,^2\Pi(3p\pi)$ state with electron configuration $1\sigma^2 2\sigma^2 3\sigma^2 4\sigma^2 5\sigma^2 1\pi^4 3\pi$ were obtained using the improved virtual orbital (IVO) method[46] with a fully relaxed core for the $X\,^1\Sigma^+$ ion. Note here and below that we use the molecular orbital $(6\sigma,7\sigma,3\pi)$ and united-atom $(3s\sigma,3p\sigma,3p\pi)$ designations interchangeably. We used a basis of $(9s5p/5s3p)$ contracted Cartesian Gaussian functions[47] augmented with one s, one p, and one d polarization function centered on the nuclei (with exponents 0.1, 0.08, and 1.0 at the N atom and 0.12, 0.09, and 1.0 at the O atom, respectively) and six s, six p, and four d diffuse functions at the center-of-mass (c.m.) with exponents 0.0453, 0.011 41, 0.005 89, 0.002 09, 0.001 016, and 0.000 387 for the s functions, 0.044, 0.0167, 0.008 13, 0.002 73, 0.001 06, and 0.000 31 for the p, and 0.1626, 0.0569, 0.0289, and 0.008 46 for the d. This basis gives calculated total energies of $-129.045\,18$ a.u. for the $D\,^2\Sigma^+$ state and $-129.044\,934$ a.u. for the $C\,^2\Pi$ state at $R=2.0069$ bohr. The single-center expansion of the 7σ orbital around the c.m. gives 0.62%s, 98.77%p, 0.47%d, and 0.07%f character, respectively, which agrees well with previous calculations.[5,7,29] A partial wave decomposition of the 3π orbital about the c.m. gives 98.98%p, 0.56%d, 0.37%f, and 0.04%g character, respectively. The photoelectron orbitals required in this study were obtained using the iterative Schwinger method in the frozen-core approximation.[48]

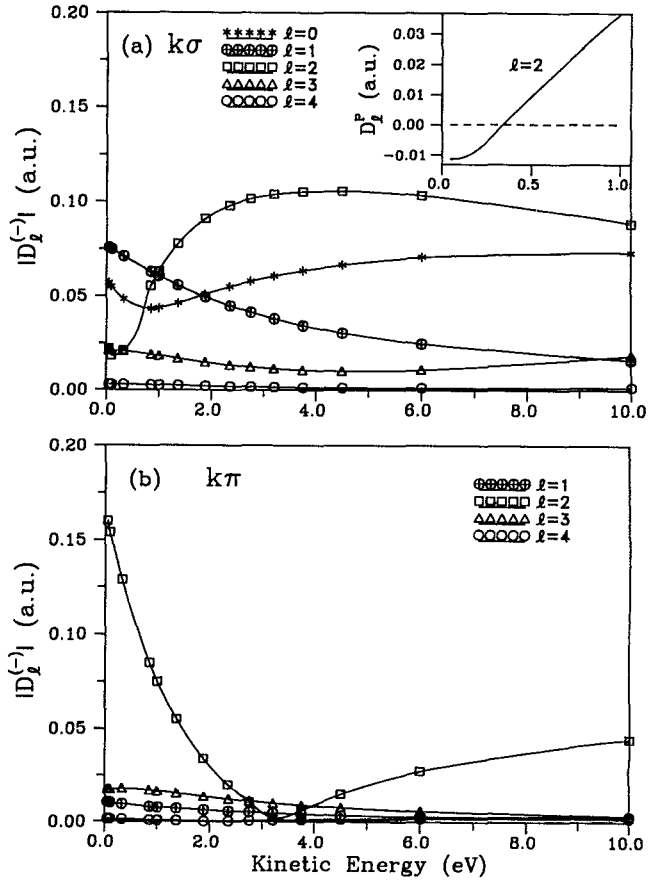

FIG. 1. Magnitude $|D_l^{(-)}|$ of the partial wave photoionization matrix elements as a function of kinetic energy for the (a) $3p\sigma\rightarrow k\sigma$ and (b) $3p\sigma\rightarrow k\pi$ channels for the $D\,^2\Sigma^+$ state. The inset shows the principal-part dipole amplitude D_l^P for the $l=2$ component.

III. RESULTS AND DISCUSSION

A. Dipole matrix elements and Cooper minima

In Fig. 1, we show the magnitude $|D_l^{(-)}|$ of the incoming-wave normalized partial wave dipole amplitude as a function of photoelectron kinetic energy for photoionization channels $3p\sigma\rightarrow k\sigma$ [Fig. 1(a)] and $3p\sigma\rightarrow k\pi$ [Fig. 1(b)] via the $D\,^2\Sigma^+(3p\sigma)$ intermediate state. Two Cooper minima, which are due to sign changes in the $l=2$ (d-wave) components around the minimum in $|D_l^{(-)}|$, are clearly seen at low kinetic energy ~ 0.33 eV in the $3p\sigma\rightarrow k\sigma$ channel [Fig. 1(a)], as well as at larger kinetic energy ~ 3.2 eV in the $3p\sigma\rightarrow k\pi$ channel [Fig. 1(b)]. The actual sign changes in the matrix elements are revealed by examining[36] the principal-part (standing-wave normalized) dipole amplitude D_l^P as shown in the inset of Fig. 1(a) for the $l=2$ wave. Here the first radial node of the $l=2$ continuum wave occurs near the maximum of the outermost loop of the $3p\sigma$ Rydberg orbital, resulting in cancellations in contributions to the photoionization matrix elements. These molecular Cooper minima for excited states are similar to the atomic $3p\rightarrow kd$ Cooper minimum observed in ground state photoionization of rare gas atoms[30–32] and photoionization of excited states of heavier atoms.[33] For excited (Rydberg) states, the Cooper minima occur at much lower kinetic energy than that typically observed from the ground state due to the outward displacement of the radial node of the Rydberg orbital. The Cooper minima in the $k\sigma$ and $k\pi$ channels occur at quite different kinetic energies because the greater penetration of the $k\sigma$ photoelectron orbital induces a stronger l mixing by the nonspherical molecular potential. The dominant $l=1$ (p-wave) component near threshold in the $k\sigma$ channel [Fig. 1(a)] indicates strong l mixing which cannot be accounted for by atomiclike selection rules. The nearly pure p-wave character (98.77%) of the $D\,^2\Sigma^+(3p\sigma)$ state would predict predominant s- and d-wave contributions to the photoelectron matrix element. Note that in the case of REMPI via the $H\,^2\Sigma^+(3d,4s)$ state,[40] the predicted Cooper minima occur at nearly the same photoelectron kinetic energies in both the $k\sigma$ and $k\pi$ channels due to similar l mixing in both channels and a lack of predominant odd waves in either channel over the relevant energy range.

In Fig. 2, we show $|D_l^{(-)}|$ for the $3s\sigma\rightarrow k\sigma$ and $3s\sigma\rightarrow k\pi$ photoionization channels via the $A\,^2\Sigma^+(3s\sigma)$ state. In contrast to the $D\,^2\Sigma^+(3p\sigma)$ state, no evidence of Cooper minima is observed within the kinetic energy range studied. The 6σ orbital is nearly pure $3s$ (94%) character. It is therefore more difficult to form a Cooper minimum because of the two nodes in the radial wave function. However, Cooper minima may occur in the discrete region of excitation via transitions

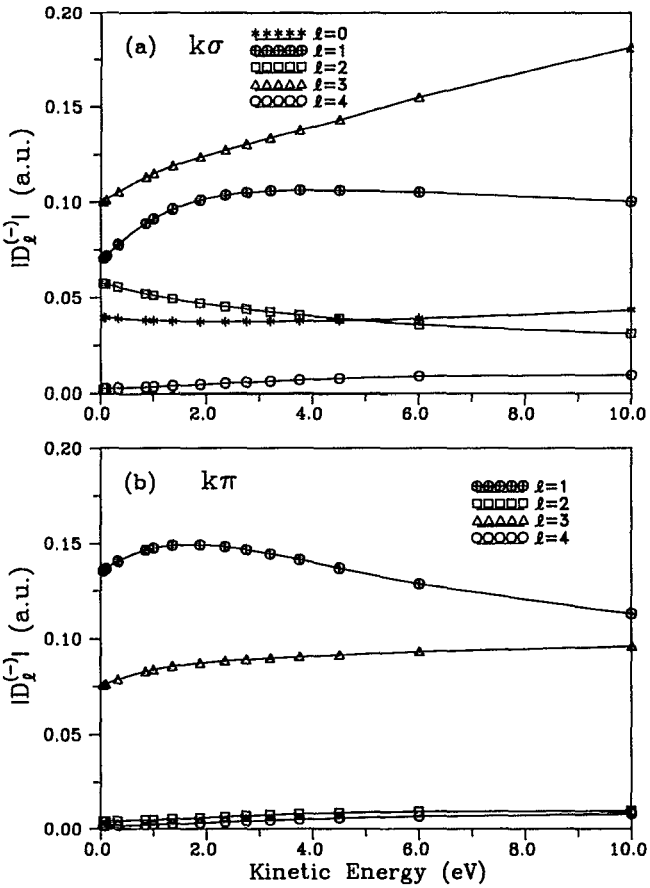

FIG. 2. The same as in Fig. 1 except for the $3s\sigma$ orbital of the $A\,^2\Sigma^+$ state.

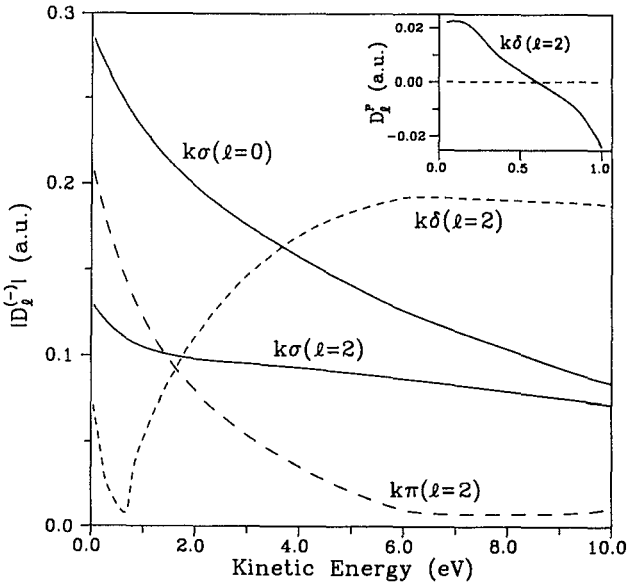

FIG. 3. $|D_l^{(-)}|$ as a function of kinetic energy for photoionization of the $C\,^2\Pi$ state. Only the dominant partial waves are shown. The inset shows the principal-part dipole amplitude D_l^P for the $l=2$ component of the $k\delta$ channel.

to highly excited Rydberg states.[41] A Cooper minimum in optical–optical double resonance spectra for Rydberg–Rydberg transitions in NO via the $C\,^2\Pi$ state has been identified and discussed by Fredin *et al.*[41]

In Fig. 3, we show $|D_l^{(-)}|$ and $D_{l=2}^P$ as a function of photoelectron kinetic energy for photoionization of the NO $C\,^2\Pi$ Rydberg state. A Cooper minimum is predicted to occur ~ 0.61 eV in the $3p\pi \rightarrow k\delta(l=2)$ channel as reflected in a sign change in D_l^P. The odd partial wave contributions are not shown in Fig. 3 because of their small amplitude. The influence of these Cooper minima on ion rotational distributions will be discussed in the following sections.

B. REMPI spectra via the $D\,^2\Sigma^+(3p\sigma)$ Rydberg state

In Fig. 4, we compare our calculated photoelectron spectra (right-hand side) with the experimental spectra[4] (left-hand side) for (2 + 1) REMPI of NO via the S_{21} (11.5) rotational branch of the 0–0 band of the $X \rightarrow D$ transition. The spectra for photoelectron detection parallel and perpendicular to the polarization vector of the radiation are shown in Figs. 4(a) and 4(b), respectively. The alignment of the $D\,^2\Sigma^+$ $(v=0, N=14)$ state created by the two-photon excitation can be determined by the 3-j symbol of Eq. (4) for this S_{21} rotational branch. The calculated spectra are convoluted with a Gaussian detector function having a full-width at half-maximum (FWHM) of 6 meV, chosen as representative of the actual experimental resolution. Agreement

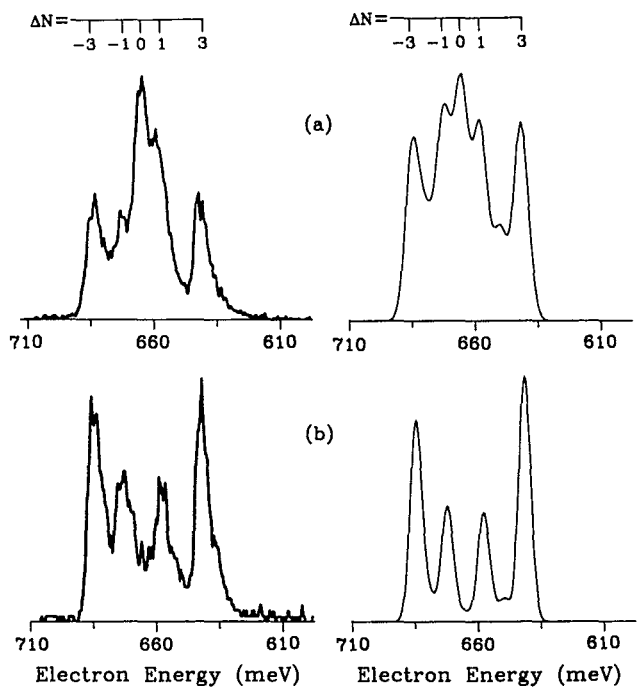

FIG. 4. Experimental (left-hand side) and calculated (right-hand side) photoelectron spectra with the laser tuned to the S_{21} (11.5) line of the $X \rightarrow D$ transition of NO for (a) laser light polarized parallel to photoelectron detection; (b) laser light polarized perpendicular to photoelectron detection. The calculated spectra are convoluted with a Gaussian detector function with an FWHM of 6 meV.

between the calculated and experimental spectra is quite good for both parallel and perpendicular detections. The $\Delta N = 0$ peaks have the strongest intensity in both the calculated and measured ion rotational distributions for photoelectron detection parallel to the laser polarization. In a previous study by Rudolph *et al.*,[21,22] the $\Delta N = 0$ signal was significant, but somewhat weaker than observed in the experiment.[4] The differences between these calculations is due to our use here of a more extensive basis including diffuse Gaussian d functions at the center of mass. The calculated ion rotational distributions in the vicinity of a Cooper minimum can be very sensitive to the inclusion of such basis functions. Examination of $|D_l^{(-)}|$ for the $D\,^2\Sigma^+$ state (Fig. 1) shows that the Cooper minimum in the $3p\sigma \rightarrow k\sigma (l = 2)$ channel *plays an essential role* in the occurrence of the $\Delta N = 0$ peak, since depletion of the $l = 2$ wave enhances the relative importance of the $l = 1$ partial wave in its vicinity. The Cooper minimum in the $3p\sigma \rightarrow k\pi (l = 2)$ channel may also affect the $\Delta N = 0$ signal, however, it is not as significant as that of the $k\sigma$ channel due to the weaker odd waves in the continuum and occurrence of the minimum at higher kinetic energy.

Figure 5 depicts the photoelectron spectra with the laser polarized parallel and perpendicular to the flight direction for $(2 + 1')$ REMPI via the S_{21} (11.5) rotational branch at several photoelectron kinetic energies. The integrated photoionization cross sections, suitable for comparison with results obtained using the time-of-flight technique equipped with a magnetic bottle apparatus,[49] are also shown. The range of kinetic energies is chosen to illustrate the effect of both Cooper minima (see Fig. 1). The ionic rotational branching ratios are strongly dependent on photoelectron kinetic energy due to the changes in the partial wave composition in the matrix elements $D_l^{(-)}$ around the Cooper minima. In Fig. 6, we show the photoelectron angular distributions corresponding to the $\Delta N = 0$–3 transitions of the rotational branching ratios of Fig. 5. All transitions for negative ΔN have similar angular distributions compared with the corresponding positive ΔN (not shown). The photoelectron angular distributions for the $\Delta N = 0$ transitions reflect the p-wave character over the entire energy range as seen in Fig. 6. The changes in the angular distributions for $\Delta N = \pm 1$ transitions as a function of photoelectron kinetic energy reflect the variation in the partial wave components of the photoelectron matrix elements in the vicinity of the Cooper minima.

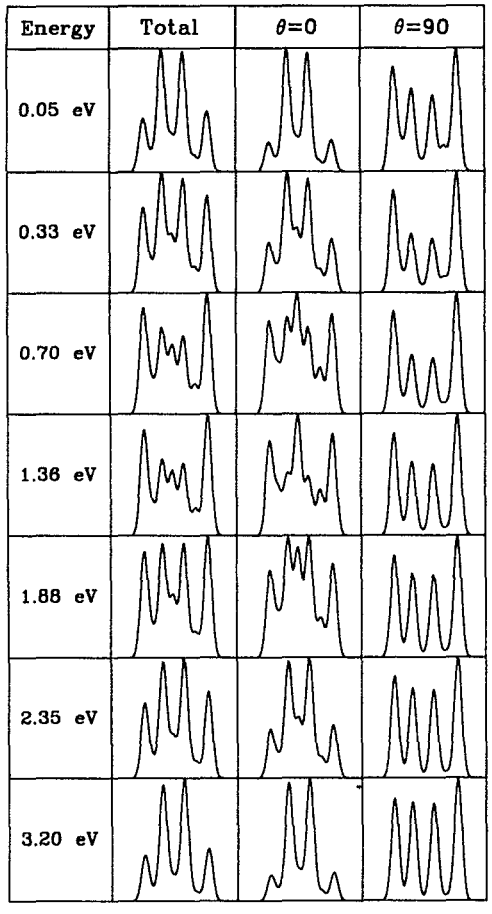

FIG. 5. Photoelectron spectra with laser tuned to the S_{21} (11.5) line of the $X \rightarrow D$ transition at several photoelectron kinetic energies for (i) the total cross section; (ii) laser light polarized parallel ($\theta = 0°$); and (iii) perpendicular ($\theta = 90°$) to photoelectron detection. Each transition is convoluted with a Gaussian detector function with an FWHM of 6 meV.

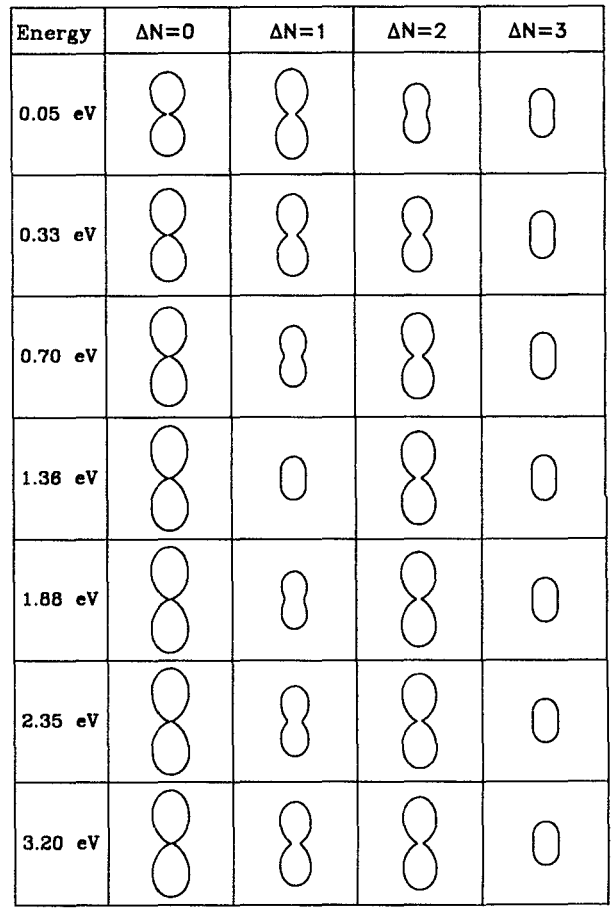

FIG. 6. Photoelectron angular distributions corresponding to the $\Delta N = 0$–3 signals of Fig. 5. Others are the same as in Fig. 5. $\theta = 0°$ is vertical.

C. REMPI spectra via the $C\,^2\Pi(3p\pi)$ Rydberg state

Photoelectron spectra for $(2+1)$ REMPI of NO via the $C\,^2\Pi(3p\pi)$ state were originally studied by Viswanathan *et al.*[5] A $\Delta N = \pm 1, \pm 3$ propensity was observed when ionizing from the $+$ parity (f) of $J = 13.5 (N = 14)$ of the C state, whereas ionization from the $-$ parity (e) of the same J level yields a $\Delta N = 0, \pm 2$ propensity. Here the e level refers to the level with parity $+(-1)^{J-1/2}$ and the f level refers to the level with parity $-(-1)^{J-1/2}$.[50] The Λ doublets of the $X\,^2\Pi$ and $C\,^2\Pi$ states result in a separation of $\sim 4\ \mathrm{cm}^{-1}$ between the Q_{21} (13.5) *ee* and *ff* rotational lines.[5] The photoelectron spectra show that the $C\,^2\Pi$ state is essentially unperturbed by the $B\,^2\Pi$ state for higher J levels,[51] whereas the ZEKE-REMPI study for low J levels reveals a strong perturbation.[10] An *ab initio* calculation, based on the pure C state, has confirmed the observed propensities.[42] Here we show results which illustrate the effects of the Cooper minimum on these photoelectron spectra. Figures 7 and 8 show photoelectron spectra for $(2+1')$ REMPI via the Q_{21} (13.5) *ee* and *ff* rotational lines of the $X \rightarrow C$ transition, respectively, at several photoelectron kinetic energies. The alignments of the $C\,^2\Pi$ state via the *ee* and *ff* lines were determined from Eq. (5) by including six $^2\Sigma^+$, four $^2\Pi$, and two $^2\Delta$ virtual states (obtained from IVO calculations) and using the intermediate coupling scheme in evaluating the B_2 and B_0 factors of Eq. (5). Surprisingly, only a small change in the rotational ion distribution is apparent throughout the energy range. The photoelectron spectra are not strongly

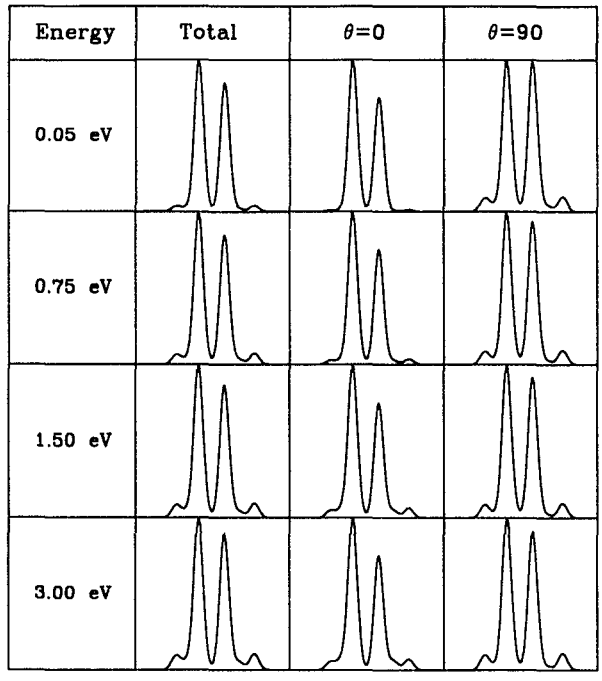

FIG. 8. The same as in Fig. 7 except that the first laser is tuned to the Q_{21} (13.5) *ff* line of the $X \rightarrow C$ transition. The dominant peaks from left to right correspond to $\Delta N = -3, -1, 1$, and 3 transitions, respectively.

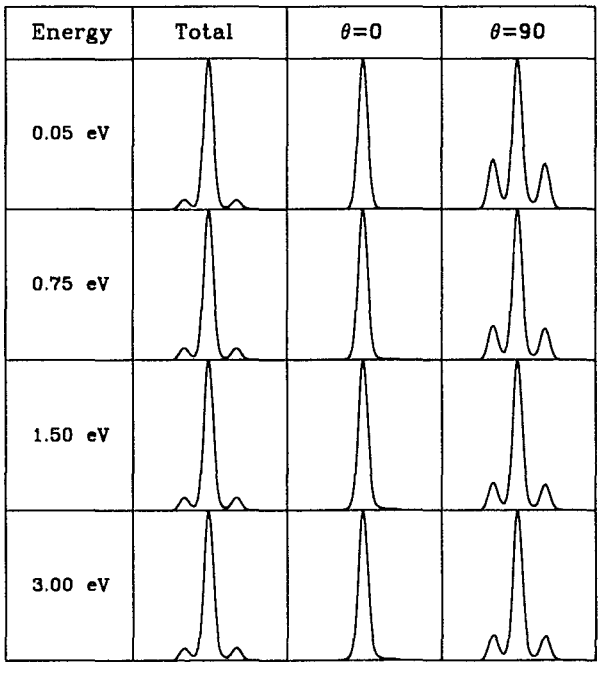

FIG. 7. Photoelectron spectra of the $(2+1')$ REMPI with laser tuned to the Q_{21} (13.5) *ee* line of the $X \rightarrow C$ transition at several electron kinetic energies. The dominant peaks from left to right correspond to $\Delta N = -2, 0$, and 2 transitions, respectively. Other designations are the same as in Fig. 5.

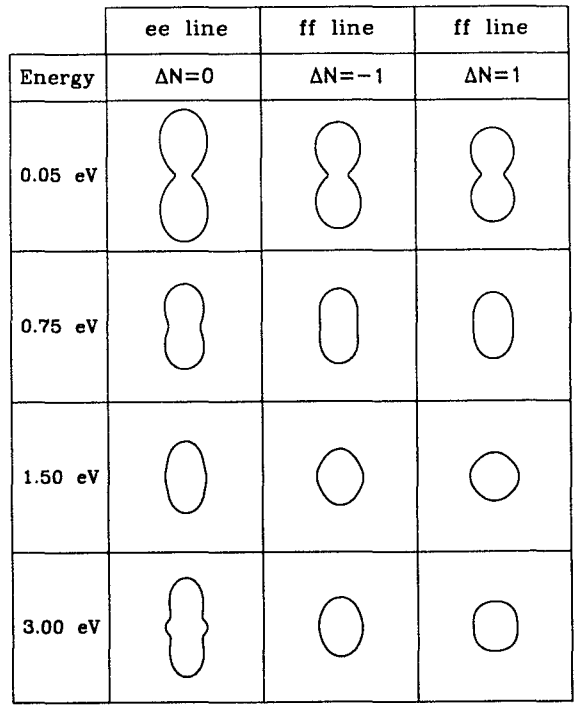

FIG. 9. Photoelectron angular distributions for the $\Delta N = 0$ transition of the *ee* line of Fig. 8 and those for $\Delta N = \pm 1$ of the *ff* line of Fig. 8. $\theta = 0°$ is vertical.

dependent on the presence of the Cooper minimum in the $3p\pi \rightarrow k\delta(l=2)$ channel because other partial waves associated with the $k\sigma$ and $k\pi$ channels dominate near threshold (Fig. 3). The atomiclike behavior of the C state (i.e., small odd-wave contributions) also leads to this result. However, the photoelectron angular distributions, shown in Fig. 9, are *strongly* dependent on the kinetic energy, due to the interference of alternative dipole amplitudes $D_l^{(-)}$ with the $3p\pi \rightarrow k\delta(l=2)$ channel exhibiting the Cooper minimum.

ACKNOWLEDGMENTS

This work was supported by grants from the National Science Foundation (CHE-8521391), Air Force Office of Scientific Research (Contract No. 87-0039), and the Office of Health and Environmental Research of the U.S. Department of Energy (DE-FG03-87ER60513). We also acknowledge use of resources of the JPL/Caltech CRAY X-MP/18 Supercomputer.

[1] R. N. Compton and J. C. Miller, in *Laser Applications in Physical Chemistry*, edited by D. K. Evans (Dekker, New York, 1988).
[2] K. Kimura, Int. Rev. Phys. Chem. **6**, 195 (1987).
[3] S. T. Pratt, P. M. Dehmer, and J. L. Dehmer, in *Advances in Multiphoton Processes and Spectroscopy*, edited by S. H. Lin (World Scientific, Singapore, 1988), and the references and tabulation of REMPI-PES studies therein.
[4] W. G. Wilson, K. S. Viswanathan, E. Sekreta, and J. P. Reilly, J. Phys. Chem. **88**, 672 (1984).
[5] K. S. Viswanathan, E. Sekreta, E. R. Davidson, and J. P. Reilly, J. Phys. Chem. **90**, 5078 (1986).
[6] K. S. Viswanathan, E. Sekreta, and J. P. Reilly, J. Phys. Chem. **90**, 5658 (1986).
[7] X. Song, E. Sekreta, J. P. Reilly, H. Rudolph, and V. McKoy, J. Chem. Phys. **91**, 6062 (1989).
[8] S. W. Allendorf, D. J. Leahy, D. C. Jacobs, and R. N. Zare, J. Chem. Phys. **91**, 2216 (1989).
[9] K. Müller-Dethlefs, M. Sander, and E. W. Schlag, Chem. Phys. Lett. **112**, 291 (1984).
[10] M. Sander, L. A. Chewter, K. Müller-Dethlefs, and E. W. Schlag, Phys. Rev. A **36**, 4543 (1987).
[11] M. G. White, M. Seaver, W. A. Chupka, and S. D. Colson, Phys. Rev. Lett. **49**, 28 (1982).
[12] S. L. Anderson, G. D. Kubiak, and R. N. Zare, Chem. Phys. Lett. **105**, 22 (1984).
[13] S. T. Pratt, P. M. Dehmer, and J. L. Dehmer, J. Chem. Phys. **78**, 4315 (1983); **79**, 3234 (1983); **81**, 3444 (1984); **92**, 262 (1990).
[14] S. T. Pratt, P. M. Dehmer, and J. L. Dehmer, Chem. Phys. Lett. **105**, 28 (1984).
[15] J. C. Miller and R. N. Compton, J. Chem. Phys. **75**, 2020 (1981); **84**, 675 (1986).
[16] S. T. Pratt, E. D. Poliakoff, P. M. Dehmer, and J. L. Dehmer, Chem. Phys. **78**, 65 (1983).
[17] S. T. Pratt, E. F. McCormack, J. L. Dehmer, and P. M. Dehmer, J. Chem. Phys. **92**, 1831 (1990).
[18] M. A. O'Halloran, S. T. Pratt, P. M. Dehmer, and J. L. Dehmer, J. Chem. Phys. **87**, 3288 (1987).
[19] P. J. Miller, L. Li, W. A. Chupka, and S. D. Colson, J. Chem. Phys. **89**, 3921 (1988).
[20] S. N. Dixit, D. L. Lynch, V. McKoy, and W. M. Huo, Phys. Rev. A **32**, 1267 (1985).
[21] H. Rudolph, S. N. Dixit, V. McKoy, and W. M. Huo, Chem. Phys. Lett. **137**, 521 (1987).
[22] H. Rudolph, S. N. Dixit, V. McKoy, and W. M. Huo, J. Chem. Phys. **88**, 637 (1988).
[23] H. Rudolph, S. N. Dixit, V. McKoy, and W. M. Huo, J. Chem. Phys. **88**, 1516 (1988).
[24] H. Rudolph, V. McKoy, and S. N. Dixit, J. Chem. Phys. **90**, 2570 (1989).
[25] H. Rudolph and V. McKoy, J. Chem. Phys. **91**, 2235 (1989).
[26] S. N. Dixit and V. McKoy, Chem. Phys. Lett. **128**, 49 (1986).
[27] J. Xie and R. N. Zare, J. Chem. Phys. **93**, 3033 (1990).
[28] K. Wang and V. McKoy, J. Chem. Phys. (in press).
[29] K. Haufman, C. Nager, and M. Jungen, Chem. Phys. **95**, 385 (1985).
[30] J. W. Cooper, Phys. Rev. **128**, 681 (1962).
[31] U. Fano and J. W. Cooper, Rev. Mod. Phys. **40**, 441 (1968).
[32] A. F. Starace, in *Handbuch der Physik*, edited by M. Mehlhorn (Springer, Berlin, 1982), Vol. 31, pp. 1–121.
[33] S. T. Manson, Phys. Rev. A **31**, 3698 (1985); A. Z. Msezane and S. T. Manson, Phys. Rev. Lett. **48**, 473 (1982).
[34] T. A. Carlson, M. O. Krause, W. A. Svensson, P. Gerard, F. A. Grimm, T. A. Whitley, and B. P. Pullen, Z. Phys. D **2**, 309 (1986).
[35] J. A. Stephens and V. McKoy, Phys. Rev. Lett. **62**, 889 (1989).
[36] J. A. Stephens and V. McKoy, J. Chem. Phys. **93**, 7863 (1990).
[37] K. Wang, J. A. Stephens, and V. McKoy, J. Chem. Phys. **93**, 7874 (1990).
[38] E. de Beer, C. A. de Lange, J. A. Stephens, K. Wang, and V. McKoy, J. Chem. Phys. **95**, 714 (1991).
[39] H. Rudolph, R. L. Dubs, and V. McKoy, J. Chem. Phys. **93**, 7513 (1990).
[40] H. Rudolph and V. McKoy, J. Chem. Phys. **91**, 7995 (1989); **93**, 7054 (1990).
[41] S. Fredin, D. Gauyacq, M. Horani, C. Jungen, G. Lefevre, and F. Masnou-Seeuws, Mol. Phys. **60**, 825 (1987).
[42] K. Wang, H. Rudolph, and V. McKoy (to be published).
[43] K. P. Huber and G. Herzberg, *Molecular Spectra and Molecular Structure. IV. Constants of Diatomic Molecules* (Van Nostrand Reinhold, New York, 1979).
[44] M. Dubs, U. Bruhlmann, and J. R. Huber, J. Chem. Phys. **84**, 3106 (1986).
[45] J. B. Halpern, H. Zacharias, and R. Wallenstein, J. Mol. Spectrosc. **79**, 1 (1980).
[46] W. J. Hunt and W. A. Goddard, Chem. Phys. Lett. **3**, 414 (1969).
[47] T. H. Dunning, J. Chem. Phys. **53**, 2823 (1970).
[48] R. R. Lucchese, G. Raseev, and V. McKoy, Phys. Rev. A **25**, 2572 (1982).
[49] P. Kruit and F. H. Read, J. Phys. E **16**, 313 (1983).
[50] J. M. Brown, J. T. Hougen, K. P. Huber, J. W. C. Johns, I. Kopp, H. Lefebvre-Brion, A. J. Merer, D. A. Ramsay, J. Rostas, and R. N. Zare, J. Mol. Spectrosc. **55**, 500 (1975).
[51] E. Miescher, J. Mol. Spectrosc. **53**, 302 (1974).